Electroacupuncture attenuates depressive-like behaviors in poststroke depression mice through promoting hippocampal neurogenesis and inhibiting TLR4/NF-κB/NLRP3 signaling pathway

Ming Li[a,*], Fang Yang[b,*], Xiaoling Zhang[a], Hong Yang[a], Xingjin He[a], Zhongnan Mao[a] and Liya Mao[a]

The aim of this study was to investigate the impact and underlying molecular mechanisms of electroacupuncture on mice with poststroke depression (PSD). Mice were randomly allocated into sham, PSD, and electroacupuncture groups. Mice in the PSD and electroacupuncture groups underwent middle cerebral artery occlusion (MCAO) surgery following with sedentary behavior. Electroacupuncture targeting Zusanli (ST36) acupoint was performed 24 h after MCAO for 4 weeks in electroacupuncture group. The sucrose preference test, forced swimming test, open field test, tail suspension test, elevated plus maze, Catwalk analysis, RNA sequencing, Nissl staining, Golgi staining, TUNEL staining, Edu labeling, and doublecortin staining were performed. Lymphocyte subsets in peripheral blood and the levels of IL-1β, IL-6, TNF-α, and expression of Iba1/CD86, Iba1/NLRP3, TLR4/p38/NF-κB/NLRP3 pathways in the hippocampus were detected. Electroacupuncture effectively protected against the development of depression-like symptoms. The number of granulosa cells and doublecortin-positive cells in the dentate gyrus (DG) were significantly decreased in PSD group, which were significantly upregulated ($P < 0.01$) by electroacupuncture. Electroacupuncture also significantly reduced ($P < 0.05$) TUNEL-positive cells in the DG and CA1. RNA-seq revealed that electroacupuncture may exert antidepressant effect by regulating the inflammation mediated by TLR4/NF-κB/NLRP3 pathway in hippocampus. Electroacupuncture remarkably elevated ($P < 0.01$) the ratio of CD4+ to CD8+ T cells and percentage of CD3-CD49b+ cells in CD45+CD49b+ cells in the peripheral blood. Electroacupuncture significantly reduced ($P < 0.05$) the high levels of IL-1β, IL-6, TNF-α, iba1, TLR4, p-p38, p-NF-κB, and NLRP3 and sedentary behavior. Electroacupuncture was observed to mitigate depression symptoms and increase hippocampal neurogenesis in mice with PSD, possibly by inhibiting TLR4/p38/NF-κB/NLRP3 pathways and improving the microglia-mediated inflammatory microenvironment in the hippocampus.

***NeuroReport* 35: 947–960 Copyright © 2024 The Author(s). Published by Wolters Kluwer Health, Inc.**

NeuroReport 2024, **35**:947–960

Keywords: depression, electroacupuncture, neurogenesis, neuroinflammation, stroke

[a]Department of Rehabilitation Medicine and [b]Department of Rheumatoid Orthopedics, Affiliated Hospital of Gansu University of Traditional Chinese Medicine, Lanzhou, China

Correspondence to Zhongnan Mao, Department of Rehabilitation Medicine, Affiliated Hospital of Gansu University of Traditional Chinese Medicine, 730000 Lanzhou, Gansu province, China Tel: +86 13519641937; e-mail: maozhongnan521@163.com
Liya Mao, No. 732, Jiayuguan West Road, Chengguan District, 730000 Lanzhou City, Gansu Province, China
Tel: 86 13679478370; e-mail: 113210965@qq.com

*Ming Li and Fang Yang contributed equally to the writing of this article.

Received 4 June 2024 **Accepted** 25 June 2024.

Introduction

Stroke remains the leading cause of death after cancer and cardiac disease, often resulting in mood and cognitive impairments [1]. Poststroke depression (PSD) affects approximately 31% of stroke patients, posing a significant burden on individuals, families, and society [2]. PSD patients have delayed recovery of neurological function, poor concentration, and decreased cognitive and executive ability, hindering rehabilitation effectiveness and elevating suicide and mortality rates compared to stroke alone [3]. Selective serotonin reuptake inhibitors (SSRIs) are common drugs for the first-line treatment of depression, but side effects like sleep disorders and cardiotoxicity limit their efficacy [4].

Acupuncture holds promise as a non-pharmacological alternative for reducing depression symptoms and improving therapeutic outcomes, with low cost and minimal side effects [5]. In the context of PSD, a meta-analysis revealed that acupuncture exhibited a superior efficacy over controls, leading to a reduction in PSD symptoms [6]. The evidence of the curative effectiveness of acupuncture, and research into its related molecular mechanisms in animal experiments, however, are still lacking.

This is an open-access article distributed under the terms of the Creative Commons Attribution-Non Commercial-No Derivatives License 4.0 (CCBY-NC-ND), where it is permissible to download and share the work provided it is properly cited. The work cannot be changed in any way or used commercially without permission from the journal.

Despite extensive use of animal depression models, depression is multifaceted, involving diverse characteristics and pathophysiological processes like neuroplasticity and inflammation [7]. Depression-induced changes in synaptic plasticity are associated with structural and functional changes in the hippocampus. Reduced hippocampal volumes may be a neural scar marker of depression and a vulnerability marker for future episodes [8]. In recent years, an increasing amount of literatures have reported that inflammation is linked with depression [9,10]. Previous research revealed that chronic stress mediates the activation of toll-like receptor 4 (TLR4) in the brain. The sustained expression of TLR4 can induce neuroinflammation, which contributes to psychiatric disorders. Activation of the TLR4 complex might underlie the pathophysiology of stress-evoked depression [11]. Activated TLR4 can induce phosphorylation of the nuclear factor-κB (NF-κB) through the myeloid differentiation primary response 88 (Myd88) adaptor, and enhances expression of inflammation cytokines, such as IL-1β, IL-6, IL-15, and IL-27 [12]. Previous studies have indicated that acupuncture has the potential to increase hippocampal and network neuroplasticity and decrease brain inflammation. Whether acupuncture can improve the symptoms of PSD by improving the inflammatory environment in the hippocampus and thus affecting its neuroplasticity, however, is unknown.

In this study, we evaluated the effect of electroacupuncture treatment at Zusanli (ST36) in a rodent model of PSD through multiple behavioral tests. Furthermore, we analyzed hippocampal neuroplasticity and inflammatory immune response as related mechanisms, measured by Nissl staining, Edu labeling, doublecortin staining, RNA sequencing and bioinformatics analysis, flow cytometry, respectively. Additionally, we verified the role of TLR4 signaling pathway in the improvement of PSD by electroacupuncture.

Materials and methods

Animals

Healthy 8-week-old male C57BL/6J mice from Beijing Vital River Laboratory Animal Technology Co., Ltd., China were acclimatized for 1 week in a setting at 22 ± 2°C, 50–60% humidity, and a 12-h light-dark cycle (lights on 7 a.m. to 7 p.m.). All experimental procedures were conducted in adherence to NIH guidelines and local ethics. Mice (n = 65) were randomized into sham (n = 15), PSD (n = 15), and electroacupuncture (electroacupuncture, n = 15) groups presurgery. Both PSD and electroacupuncture groups have undergone PSD modeling. Overall, 20 mice were excluded based on the following criteria: death, extreme physical weakness, or failed surgery. The timeline diagram of experimental protocols was showed in Fig. 1a.

Modeling of poststroke depression

The PSD model was established through middle cerebral artery occlusion (MCAO) surgery followed by postoperative restraint activities. Briefly, the mice in the PSD and electroacupuncture groups were deeply anesthetized with 1% pentobarbital sodium (1 ml/100 g, i.p.) and then to expose the left common carotid artery (CCA), external carotid artery (ECA), and internal carotid artery (ICA). The ECA was ligated, dissected, and inserted gently with a round-tip nylon thread (Beijing Cinontech Co. Ltd, China), and turned into ICA to block blood flow at the middle cerebral artery (MCA). After 60 min, the thread was removed, and successful modeling was confirmed by cerebral blood flow monitoring (Fig. 1b). The sham group mice, like the PSD and electroacupuncture group mice, underwent anesthesia and neck incision surgery, but without MCA occlusion. The purpose of setting up a sham surgery group is to exclude the potential impact of chronic inflammation caused by surgical trauma on depressive-like behavior. Postsurgery, mice were singly housed in narrow and small plastic cages (cage size: 26 × 19 × 15 cm) with food and water available *ad libitum* to restrict movement. Evaluate depressive-like behavior in mice through several behavioral experiments introduced below.

Electroacupuncture intervention

For electroacupuncture intervention, we used a G6805-2A electroacupuncture apparatus (Shanghai Huayi Co., China) targeting Zusanli (ST36) on the right affected limb. Mice in electroacupuncture group were anesthetized with isoflurane (induction with 3%; maintenance with 1.2%) in oxygen-enriched air by face mask, and rectal temperature was controlled at 37 ± 0.5°C throughout the experiment with heating lamps. A 0.3 mm diameter acupuncture needle was gently inserted to 2–3 mm depth. Disperse-dense waves of either 4 or 20 Hz were employed, with an output voltage of 4 V. The intensity of the stimulation was carefully regulated to remain slightly below the threshold needed to induce visible muscle contraction. Only electroacupuncture group mice underwent electroacupuncture intervention 24 h after MCAO surgery and lasting 30 min/day for 4 weeks until sacrifice. The mice in the sham and PSD group underwent the same anesthesia procedures as the electroacupuncture group without the electroacupuncture.

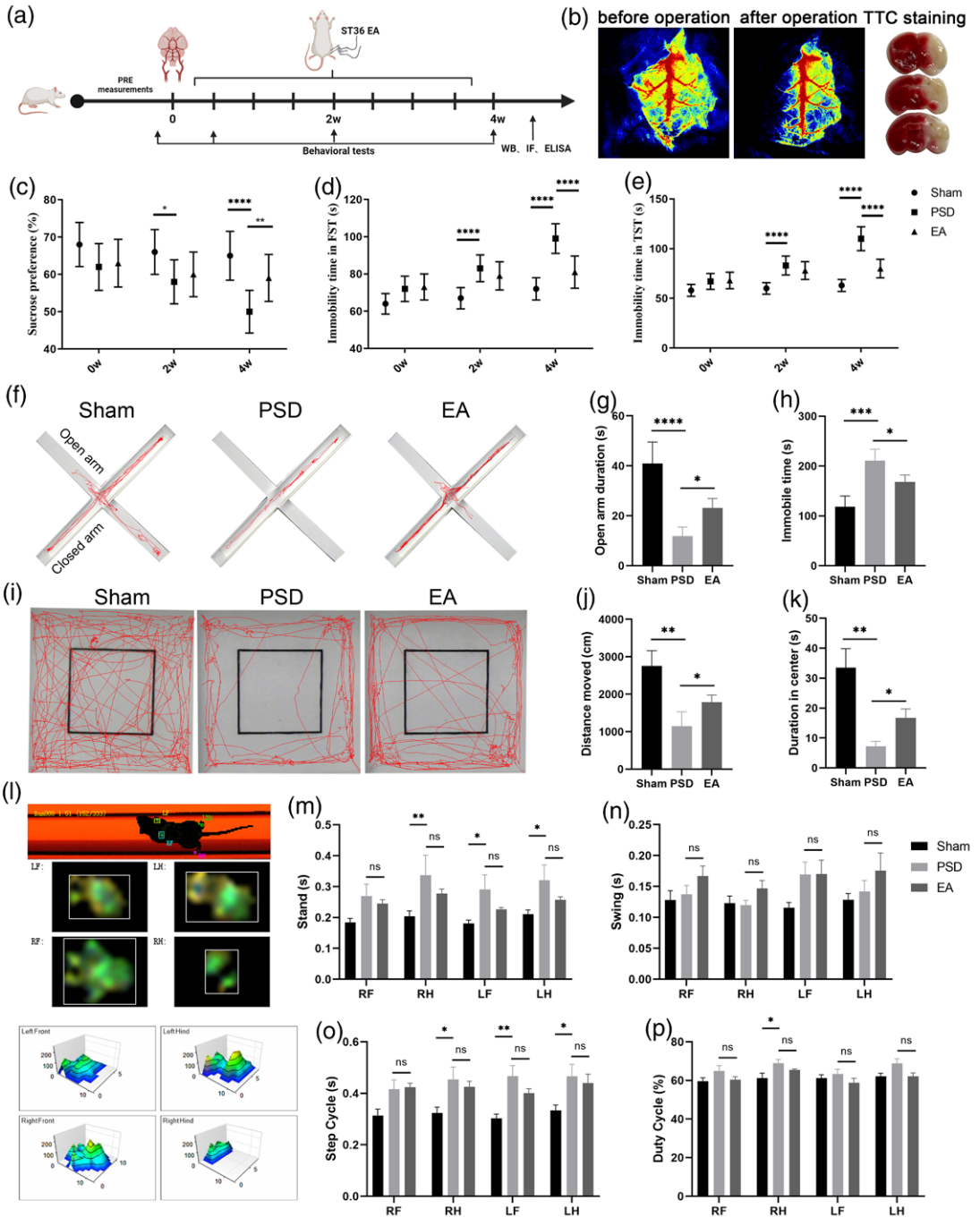
Behavioral tests

Behavioral tests included the sucrose preference test (SPT), forced swimming test (FST), tail suspension test (TST), open field test (OFT), elevated plus maze (EPM), and Catwalk analysis. These tests were performed at 1 day, 2 weeks, and 4 weeks after MCAO surgery, respectively.

Sucrose preference test

On the initial day, mice freely accessed two bottles containing 1% sucrose solution. The next day, one sucrose bottle was replaced with distilled water. On the third day, the mice were deprived of food and water for 23 h. Postdeprivation, the mice were given a preweighed bottle

Fig. 1



(a) The timeline diagram illustrates the experimental protocols. Before the MCAO as well as the 4-week period of either sedentary behavior or electroacupuncture, all mice went through an acclimatization phase for a week. Following the MCAO and the subsequent treatment, behavioral assessments were conducted. (b) The cerebral blood flow was constantly monitored by laser speckle flowmetry to set up the MCAO model. During the surgical procedure, the blood flow in the ischemic cerebral region fell to less than 30% of that in the contralateral side. (c) Comparison of the sucrose preference during SPT in each group ($n = 10$). Two-way ANOVA was used to analyze the data [$F(2,81) = 18.86$, $P < 0.001$]. (d) Comparison of the sucrose preference during FST in each group ($n = 10$). Two-way ANOVA was used to analyze the data [$F(2,81) = 44.70$, $P < 0.001$]. (e) Comparison of the sucrose preference during TST in each group ($n = 10$). Two-way ANOVA was used to analyze the data [$F(2,81) = 73.65$, $P < 0.001$]. (f–h) Comparison of the duration in open arm [one-way ANOVA, $F(2,12) = 31.92$, $P < 0.001$] and immobility time [one-way ANOVA, $F(2,12) = 23.96$, $P < 0.001$] during EPM in each group ($n = 5$). Electroacupuncture significantly increase duration in open arm and decreased immobility time. (i–k) Comparison of the distance moved [one-way ANOVA, $F(2,12) = 24.32$, $P < 0.001$] and duration in center [one-way ANOVA, $F(2,12) = 40.83$, $P < 0.001$] during OFT in each group ($n = 5$). Electroacupuncture significantly decrease distance moved and duration in center during OFT. (l–p) There were no significances in stand time, swing time, step cycle, duty cycle during gait analysis between PSD and electroacupuncture group ($n = 5$). All values are presented as means ± SD. *$P < 0.05$, **$P < 0.01$, ***$P < 0.001$, ****$P < 0.0001$.ANOVA, analysis of variance; EPM, elevated plus maze; FST, forced swimming test; MCAO, middle cerebral artery occlusion; OFT, open field test; PSD, poststroke depression; SPT, sucrose preference test; TST, tail suspension test.

of 1% sucrose solution and a bottle of distilled water. After an hour, sucrose preference (%) was calculated as sucrose consumption/(sucrose consumption + water consumption) × 100%. A decrease in sucrose preference indicated anhedonia and depression-like behavior.

Forced swimming test

Mice swam for 6 min in a transparent cylinder (37 cm diameter × 60 cm height) filled with water at a depth of 40 cm and immobility behavior during the last 5 min was measured. Immobility was characterized as the least amount of movement and struggle required for the mice to keep its head above water. Increased immobility suggested the presence of depression-like behavior.

Tail suspension test

The mouse tail was clamped in a clip and hung on a suspension rack for 6 min. The body of the mouse is 15 cm above the ground and should not come into contact with the ground or other supports. Immobility time during the last 4 min was recorded following a previously described method [13].

Open field test

The mice were then placed individually in the center of the arena and allowed to explore freely for 10 min. The behavior of the animals was recorded using video cameras mounted above the arena. Parameters such as total distance traveled, time spent in the center were measured and compared between experimental groups.

Elevated plus maze

The EPM has an open arm and a closed arm with an arm width of 5 cm, an arm length of 35 cm, a closed arm height of 15 cm, and a maze height of 50 cm above the ground. The mice were placed on the center area of the maze facing one of the open arm and allowed to explore freely for 5 min. The behavior of the animals is recorded using video cameras mounted above the arena. Parameters such as time spent in open versus closed arms, immobile time are measured and compared between experimental groups.

Catwalk analysis

Individual animals are placed at one end of the Catwalk walkway and allowed to walk freely to the other end. The high-speed camera captures the paw prints as the animal moves. Parameters such as stance duration, swing duration, step cycle are measured and compared between experimental groups.

Nissl staining and Golgi staining

Mice in each group were anesthetized with 3% isoflurane, transcardially perfused with 0.9% saline and 4.0% paraformaldehyde in PBS. Coronal sections (5 μm) at the hippocampus plane were permeabilized, and blocked with 0.3% Triton X-100 and 5% goat serum, respectively. Nissl staining involved degreasing and hydration, followed by staining in 0.1% toluidine blue solution for 20 min and differentiation in 95% ethyl alcohol for 15 min. The dentate gyrus area of the ischemic hippocampus (approximately 2 mm from bregma) was selected for photography, with four mice in each group. Quantitatively analyzed the number of entire stratum granulosa cells containing intact Nissl bodies in each single section from four mice in each group using Fiji software (NIH, USA, Bethesda). For Golgi staining, the tissue was then placed in a series of solutions that gradually impregnate it with a heavy metal salt, usually a silver compound. This process selectively deposited silver particles in the neuronal cell bodies and processes. The silver-impregnated neurons could then be visualized under Olympus Fluorview-3000 confocal microscope (Olympus Optical, Ltd., Japan, Tokyo). The dentate gyrus area of the ischemic hippocampus (about 2 mm away from bregma) was selected for photography, with four mice in each group. Fiji software (NIH) was used to perform Sholl analysis on three complete neurons in each single section from four mice in each group, and then the average number of branches and minute length of neurons were calculated.

5-Ethynyl-2'-deoxyuridine labeling, TUNEL staining, and immunofluorescence staining

Edu (250 mg/kg; Beyotime, China, Shanghai) was intraperitoneally administered once daily for 7 days before sacrifice to assess hippocampal cell proliferation. Edu staining was performed with the Edu-488 cell proliferation detection kit (Beyotime) following the manufacturer's instruction. The primary antibodies were used: NeuN (1 : 400, Proteintech, Chicago, USA), doublecortin (1 : 400, Proteintech), Iba1 (1 : 300, Wako, Japan, Tokyo), CD86 (1 : 500, Proteintech), NLRP3 (1 : 500, AdipoGen, San Diego, USA), then with secondary antibodies conjugated to Alexa Fluor (Thermo Fisher Scientific, Waltham, USA) for 1.5 h (1 : 300, Bioss, China, Beijing). Sections were observed with Olympus Fluorview-3000 confocal microscope (Olympus Optical, Ltd.). The dentate gyrus area of the ischemic hippocampus was selected for photography, and three slices were chosen at an equal distance (approximate equidistance of 666 μm) within the range from the appearance of the hippocampus (approximately 1 mm from bregma) to the disappearance of the lateral ventricle (approximately 3 mm from bregma). Quantitative analysis was conducted using Fiji software (NIH) on the number of Edu-positive cells, TUNEL-positive cells, the average fluorescence intensity of Iba1, and the colocalization ratios of iba1/CD86 and iba1/CD206 in three sections from four mice in each group.

RNA sequencing and bioinformatics analysis

Total RNA was isolated and purified using TRIzol reagent (Invitrogen, Carlsbad, USA). RNA quantity and purity were assessed with NanoDrop ND-1000. The

RNA integrity was assessed by Bioanalyzer 2100 (Agilent, Santa Clara, USA) with RNA integrity number > 7.0, and confirmed by electrophoresis with denaturing agarose gel. Poly (A) RNA was purified using Dynabeads Oligo (dT)25-61005 (Thermo Fisher, USA) and fragmented with Magnesium RNA Fragmentation Module (NEB, Massachusetts, USA). Cleaved RNA fragments were reverse-transcribed by SuperScript II Reverse Transcriptase, yielding U-labeled second-stranded DNAs. An A-base is then added to the blunt ends of each strand, preparing them for ligation to the indexed adapters. Adapters were ligated to the A-tailed DNA, and size selection was performed with AMPureXP beads. After U-labeled second-stranded DNA treatment with heat-labile UDG enzyme, ligated products were PCR-amplified. The average insert size for the final cDNA library was 300 ± 50 bp. At last, we performed the 2 × 150 bp paired-end sequencing (PE150) on an illumina Novaseq 6000 (Illumina, San Diego, USA).

Fastp software were used to remove the reads with adaptor contamination, low-quality, and undetermined bases. HISAT2 mapped reads to the reference genome of mus_musculus (GRCm38). StringTie assembled mapped reads for each sample, and all transcriptomes were merged to reconstruct a comprehensive transcriptome using gffcompare. StringTie was used to perform expression level for mRNAs by calculating FPKM [FPKM = (total_exon_fragments/mapped_reads(millions) × exon_length(kB))]. Differentially expressed mRNAs were selected with fold change >1.5 or <0.5 and parametric F-test ($P < 0.05$) using R package edgeR (AT&T BellLaboratories, Auck land, New Zealand).

Flow cytometry

To determine the percentage of total leukocytes and lymphocyte subsets, blood samples were stained with various monoclonal antibodies and evaluated by flow cytometry. Cells were analyzed on Beckton Dickinson FACS Calibur flow cytometer using flowjo software (Beckton Dickinson, New York, USA). The following antibodies were used: anti-CD4-BV510 (100449, Biolegend), anti-CD3-PE (100220, Biolegend), anti-CD8a-BV605(100744, Biolegend), anti-CD45-APC (103116, Biolegend), anti-CD19-FITC (115506, Biolegend), anti-CD49b-APC (103516, Biolegend), anti-CD11b-PE (101208, Biolegend), anti-F4/80-BV421 (123137, Biolegend, San Diego, USA). CD49b-FMO, CD11b-FMO and F4/80-FMO are required as FMO controls for setting gates.

ELISA

Protein levels of hippocampus were determined using BCA protein assay reagents. Concentrations of IL-1β, IL-6, and TNF-α were measured via ELISA kits from FANKEW (Shanghai, China), following the manufacturer's guidelines. The protein standards and samples were placed in 96-well plates and then combined with biotinylated antibodies. A microplate reader from Thermo Fisher Scientific was used to obtain the results. The concentrations were calculated based on the linear equation derived from the standard curve.

Western blotting

Hippocampal tissue from the ischemic side underwent protein extraction using RIPA lysis buffer, along with protease and phosphatase inhibitors (Beyotime). Protein concentrations were determined by BCA method (Beyotime). The extracted proteins were mixed with SDS-loading buffer (Kangwei, Beijing, China) and boiled for 10 min. Then proteins were separated by SDS-PAGE and transferred to PVDF membranes (Millipore, Boston, USA). Next, the membranes were blocked with 5% BSA for 1 h and incubated with primary antibodies against TLR4 (1 : 500, Novus, Saint Louis, USA), NF-κB/p-NF-κB (1 : 1000, CST, Boston, USA), p38/p-p38 (1 : 1000, CST), NLRP3 (1 : 1000, AdipoGen), and GAPDH (1 : 1000, Bioss) at 4°C overnight. After incubation with corresponding secondary antibodies (1 : 5000, Bioss), proteins on the membranes were detected using the ECL substrate (Tanon, Beijing, China) and visualized by UVP gel imaging system (UVP, Upland, USA). The relative band intensity was quantitative analyzed by Fiji software (NIH) and then normalized to the loading control (GAPDH).

Statistical analysis

GraphPad Prism 9.0 software (San Diego, USA) and SPSS 14.0 software (Chicago, USA) were used for statistical analysis. The results of the experiments are presented as the means with SD. The Shapiro–Wilk method is used to perform a normal distribution test on quantitative data. For data that conforms to a normal distribution, the data were analyzed statistically by one-way or two-way analysis of variance (ANOVA) for multiple comparisons followed by Tukey's or Bonferroni's post hoc test and the difference was significant at $P < 0.05$. For data that does not conform to a normal distribution, nonparametric rank sum test is used.

Results

Effects of electroacupuncture on depression-like behaviors in the sedentary mice after ischemic stroke

Our findings suggest that sedentary behavior poststroke contributes to the development of depressive behaviors, demonstrated by various tests, including the SPT, FST, TST, OPT, and EPM. Mice in the PSD group that underwent ischemic stroke and engaged in 4 weeks of sedentary behavior showed significantly reduced sucrose preference ($P < 0.0001$), indicating anhedonia or diminished pleasure responsiveness. Furthermore, in both FST, TST, EPM tests, sedentary mice poststroke in the PSD group displayed increased immobility time ($P < 0.0001$), and displayed significant decrease in exploration duration

in open arms ($P < 0.0001$) of EPM, spent time in center ($P < 0.01$) and distance moved ($P < 0.01$) of OPT. These results indicate that sedentary behavior can exacerbate depressive symptoms following a stroke.

Besides, electroacupuncture is explored as a therapeutic intervention, effectively mitigating depression-like behaviors induced by ischemic stroke with sedentary behavior. Mice in the electroacupuncture group receiving electroacupuncture showed improved sucrose preference ($P = 0.004$), exploration duration in open arms ($P = 0.023$), distance moved ($P = 0.046$), and reduced immobility time in TST ($P < 0.0001$) and FST ($P < 0.0001$). These findings highlight the potential of electroacupuncture as a treatment option for PSD, promoting overall well-being (Fig. 1c–k).

It is noteworthy that electroacupuncture did not improve the motor ability of sedentary mice after ischemic stroke. According to the results of gait analysis, there was no statistical difference ($P > 0.05$) in the stance phase duration, swing phase duration, step cycle, and duty cycle between the electroacupuncture group and the PSD group (Fig. 1l–p).

Effects of electroacupuncture on hippocampal neuroprotection in the sedentary mice after ischemic stroke

Nissl staining showed that neuronal cells in the hippocampal dentate gyrus were loosely arranged, lightly stained, or absence after ischemic stroke with sedentary behavior. Therefore, PSD group showed a significant decrease in granulosa cell count in dentate gyrus ($P < 0.0001$). Electroacupuncture for 4 weeks led to a more orderly arrangement of neuronal cells and increased granulosa cell count in dentate gyrus compared to the PSD group ($P = 0.010$; Fig. 2a and b).

According to Golgi staining, the hippocampal neurons of mice in the sham group retained intact axonal and dendritic structures, with a high density and a large number of dendritic branches ($P < 0.001$) and mean branch length ($P = 0.002$) compared with PSD group. Most of the hippocampal neurons in the PSD group mice were dead and lacked complete cellular structures. While in the electroacupuncture intervention group, the hippocampal neurons of mice retained partial axonal and dendritic structures, and the number of dendritic branches ($P = 0.010$) and length of branches ($P = 0.021$) were significantly increased compared with that in the PSD group (Fig. 2c–f).

The results of TUNEL and NeuN co-staining revealed that a significant number of neurons in the dentate gyrus and CA1 regions of the hippocampus in PSD group mice displayed positive TUNEL signals, indicating ongoing apoptosis. In comparison to the PSD group, however, the TUNEL-positive signals in the dentate gyrus ($P = 0.001$) and CA1 ($P = 0.041$) regions of the hippocampus in the electroacupuncture intervention group were significantly reduced. This finding suggests that electroacupuncture intervention has the potential to attenuate neuronal apoptosis in the hippocampus, thereby exerting a neuroprotective effect (Fig. 2g–j).

Effects of electroacupuncture on hippocampal neurogenesis in the sedentary mice after ischemic stroke

Neurogenesis plays an essential role in the recovery of brain injuries. Edu/NeuN double-labeling indicated neurogenesis in hippocampal dentate gyrus. Quantitative analysis revealed a reduction in Edu-positive cells in the PSD group compared to the sham group, while there was no significant difference between groups ($P > 0.05$). Conversely, 4-week electroacupuncture significantly increased Edu-positive cell count in dentate gyrus ($P < 0.0001$; Fig. 3a and b). Overall, the results support electroacupuncture's potential to enhance hippocampal neurogenesis in the sedentary mice after ischemic stroke.

The short-term fate of Edu-positive cells was to differentiate into neuronal precursors marked by doublecortin, which indicated immature neurons/neuronal precursors' recovery. Immunostaining of doublecortin and quantitative analysis showed a significant reduction in doublecortin-positive cells in the PSD group compared to the sham group ($P = 0.016$). In contrast, 4-week electroacupuncture significantly increased doublecortin-positive cell count in dentate gyrus compared to the PSD group ($P = 0.002$; Fig. 3c and d).

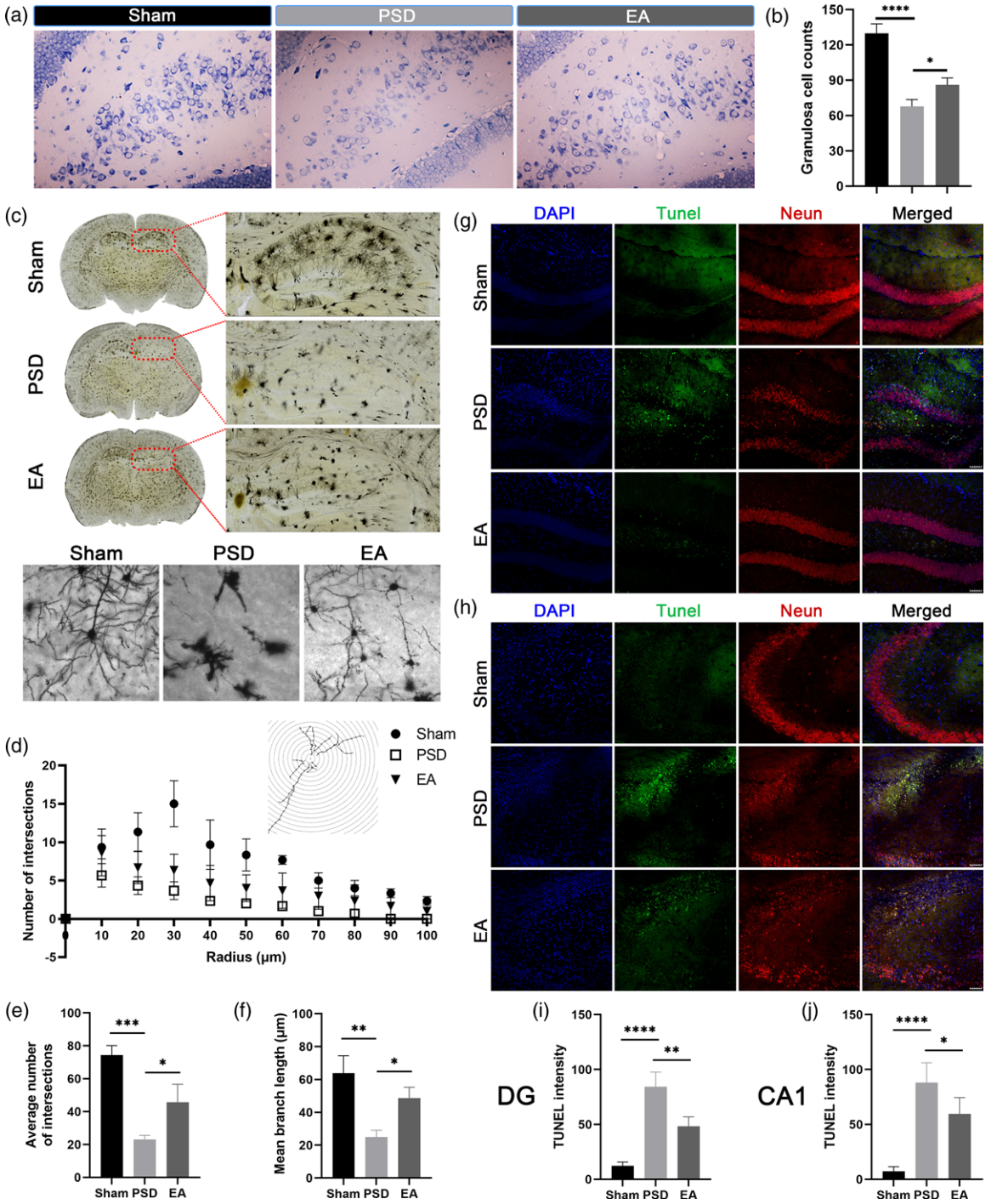
Effects of electroacupuncture on differentially expression genes in the sedentary mice after ischemic stroke

RNA sequencing unveiled 1673 differentially expressed genes in the ischemic hemisphere's hippocampus, with 125 genes upregulated and 1548 downregulated. GO annotation analysis showed that most biological-process-related genes between PSD and electroacupuncture groups were 'immune system process', 'innate immune response', 'inflammatory response', 'regulation of interleukin-6 production', and 'positive regulation of I-kappa B kinase'. KEGG enrichment analysis showed that the most significantly enriched pathways were: 'NOD-like receptor signaling pathway', 'Toll-like receptor signaling pathway', and 'NF-kappa B signaling pathway' (Fig. 4). These findings suggest that electroacupuncture might induce antidepressant effects by modulating the inflammatory response via the TLR4/NF-κB/NLRP3 signaling pathway in the hippocampus.

Effect of electroacupuncture on lymphocyte subsets and inflammatory cytokines in sedentary mice after ischemic stroke

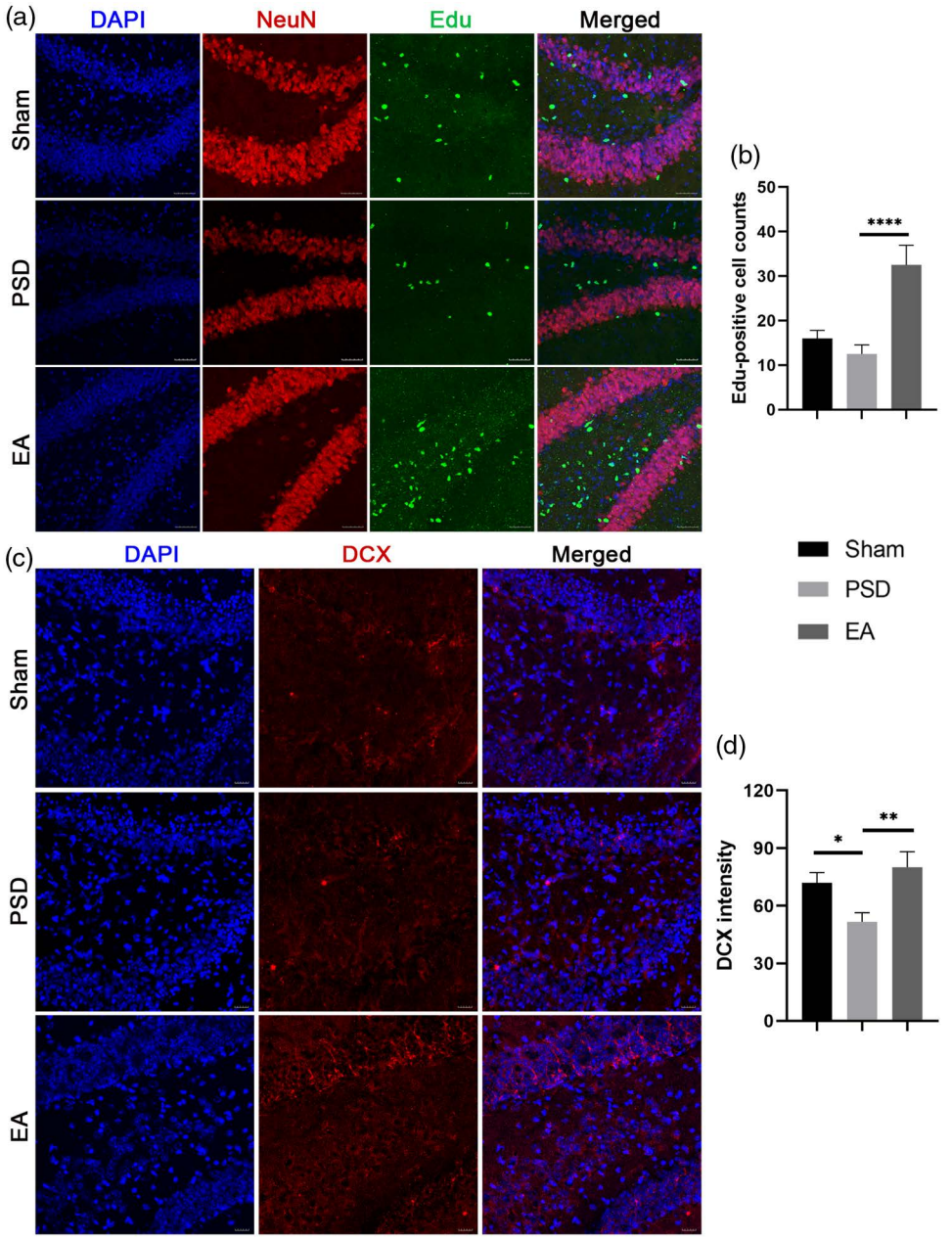
Flow cytometry analysis results showed that ischemic stroke with sedentary behavior induced a significant increase in CD8+ T cells ($P = 0.010$) and F4/80+CD11b+ cells (macrophages) ($P = 0.006$) in the peripheral blood. The percentage of CD4+ cells in CD45+CD3+ cells

Fig. 2



Effects of electroacupuncture on hippocampal neuroprotection in the sedentary mice after ischemic stroke. (a) Histological images of Nissl staining evaluated the neuronal survival in the hippocampal dentate gyrus. (b) Quantitative analysis of the number of granulosa cells ($n = 4$). One-way ANOVA was used to analyze the data [F (2,10) = 89.25, $P < 0.0001$]. (c) Histological images of Golgi staining evaluated the neuronal axonal and dendritic structures in the hippocampal dentate gyrus. (d) Sholl analysis of the complexity of the dendritic arborization of neurons, represented as dendritic intersections at a given distance from the soma. (e) Quantification of average number of intersections [$n = 4$, one-way ANOVA, F (2,10) = 36.61, $P < 0.001$]. (f) Quantification of mean dendritic length [$n = 4$, one-way ANOVA, F (2,10) = 20.01, $P = 0.002$]. Histological images of TUNEL and NeuN costaining evaluated the neuronal loss in the hippocampal dentate gyrus (d) and CA1 (e) (Scale bar = 60 μm). Quantitative analysis of the number of TUNEL-positive cells in the hippocampal dentate gyrus (f) [$n = 4$, one-way ANOVA, F (2,10) = 57.44, $P < 0.0001$] and CA1 (g) [$n = 4$, one-way ANOVA, F (2,10) = 35.19, $P < 0.0001$]. All values are presented as means ± SD. *$P < 0.05$, **$P < 0.01$, ****$P < 0.0001$. ANOVA, analysis of variance.

Fig. 3

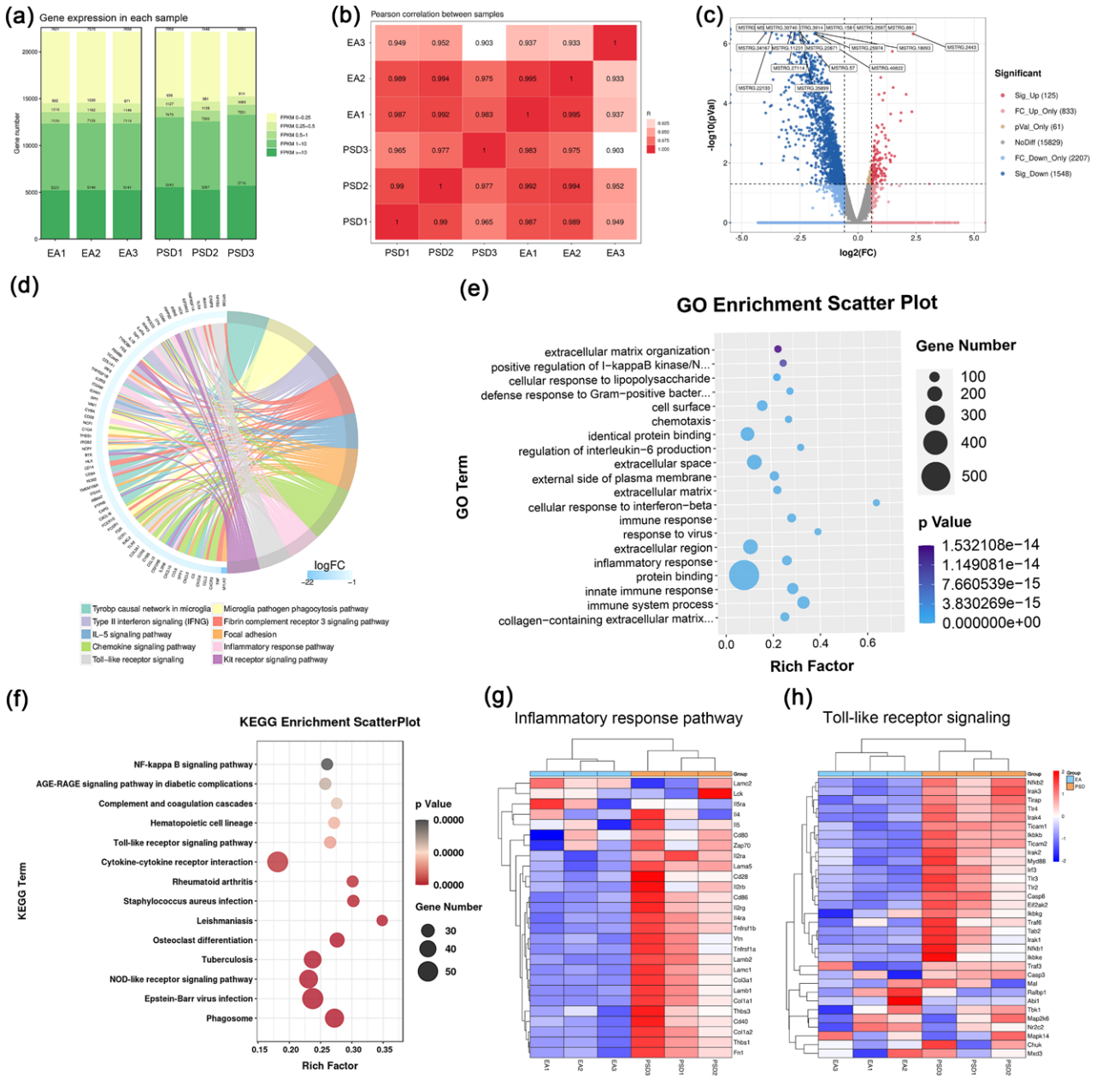


Effects of electroacupuncture on hippocampal neurogenesis in the sedentary mice after ischemic stroke. (a) Representative images of double-labeling immunostaining of Edu/NeuN (Edu-green and NeuN-red) showed the neurogenesis in hippocampal dentate gyrus (Scale bar = 60 μm). (b) Quantitative analysis of the number of Edu-positive cells in each group ($n = 4$). One-way ANOVA was used to analyze the data [F (2,10) = 50.09, $P < 0.0001$]. (c) Representative images of immunostaining of doublecortin in hippocampal dentate gyrus of ischemic side (Scale bar = 40 μm). (d) Quantitative analysis of the number of doublecortin-positive cells in dentate gyrus in each group ($n = 4$). One-way ANOVA was used to analyze the data [F (2,10) = 16.44, $P = 0.002$]. All values are presented as means ± SD. *$P < 0.05$ and **$P < 0.01$. ANOVA, analysis of variance.

($P = 0.007$), CD3-CD49b+ cells in CD45+CD49b+ cells, and the ratio of CD4+ to CD8+ cells ($P = 0.001$) significantly decreased in the PSD group compared with the sham group. Electroacupuncture for 4 weeks, however, remarkably elevated the ratio of CD4+ to CD8+ T cells and the percentage of CD3-CD49b+ cells in CD45+CD49b+ cells in the peripheral blood ($P = 0.006$; Fig. 5a–f).

In our present study, we observed a substantial increase ($P < 0.01$) in IL-1β, IL-6, and TNF-α concentrations in the ischemic hippocampus following stroke with 4 weeks of sedentary behavior. Nevertheless, electroacupuncture treatment notably decreased ($P < 0.01$) the levels of IL-1β, IL-6, and TNF-α in the affected hippocampus (Fig. 5g–i).

Fig. 4

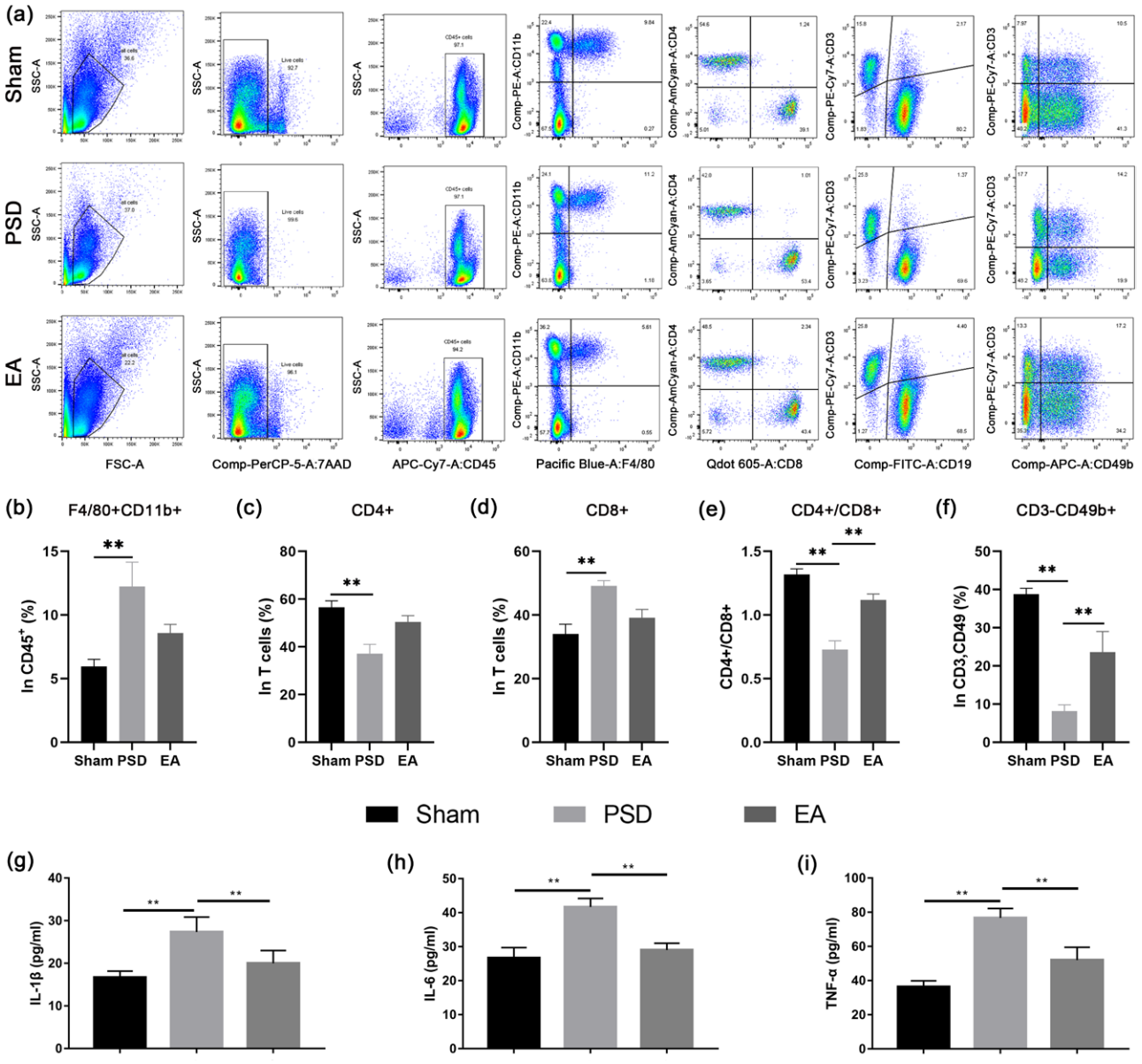


Effects of electroacupuncture on differentially expression genes in the sedentary mice after ischemic stroke. (a) Gene expression in each sample. (b) Pearson correlation between samples. (c) Volcano map of differentially expressed genes between PSD and electroacupuncture groups. There were 1673 differentially expression genes in the hippocampus of ischemic hemisphere with 125 genes upregulated and 1548 genes downregulated. (d and e) GO term enrichment analysis of differentially expressed genes. (f) KEGG pathway analysis of differentially expressed genes. (g and h) Hierarchical clustering analysis results depicting the differentially expressed genes of inflammatory response pathway and Toll-like receptor signal pathway between PSD and electroacupuncture groups. PSD, poststroke depression.

Effects of electroacupuncture on microglia-mediated neuroinflammation and TLR4/p38/NF-κB/NLRP3 signaling pathways

Glial cells, especially microglia, are widely recognized as playing a pivotal role in initiating and guiding innate immune responses in central nervous system (CNS) diseases. It is well known that the overactivation of microglia can significantly impact local inflammatory responses, leading to alterations in the neuronal microenvironment and neuronal damage [14]. Through confocal images of Iba1/CD86 ($P < 0.0001$) and Iba1/NLRP3 ($P < 0.0001$) colocalization analysis, we observed a substantial activation of proinflammatory microglia in the hippocampal region of the PSD group, which concomitantly

Fig. 5

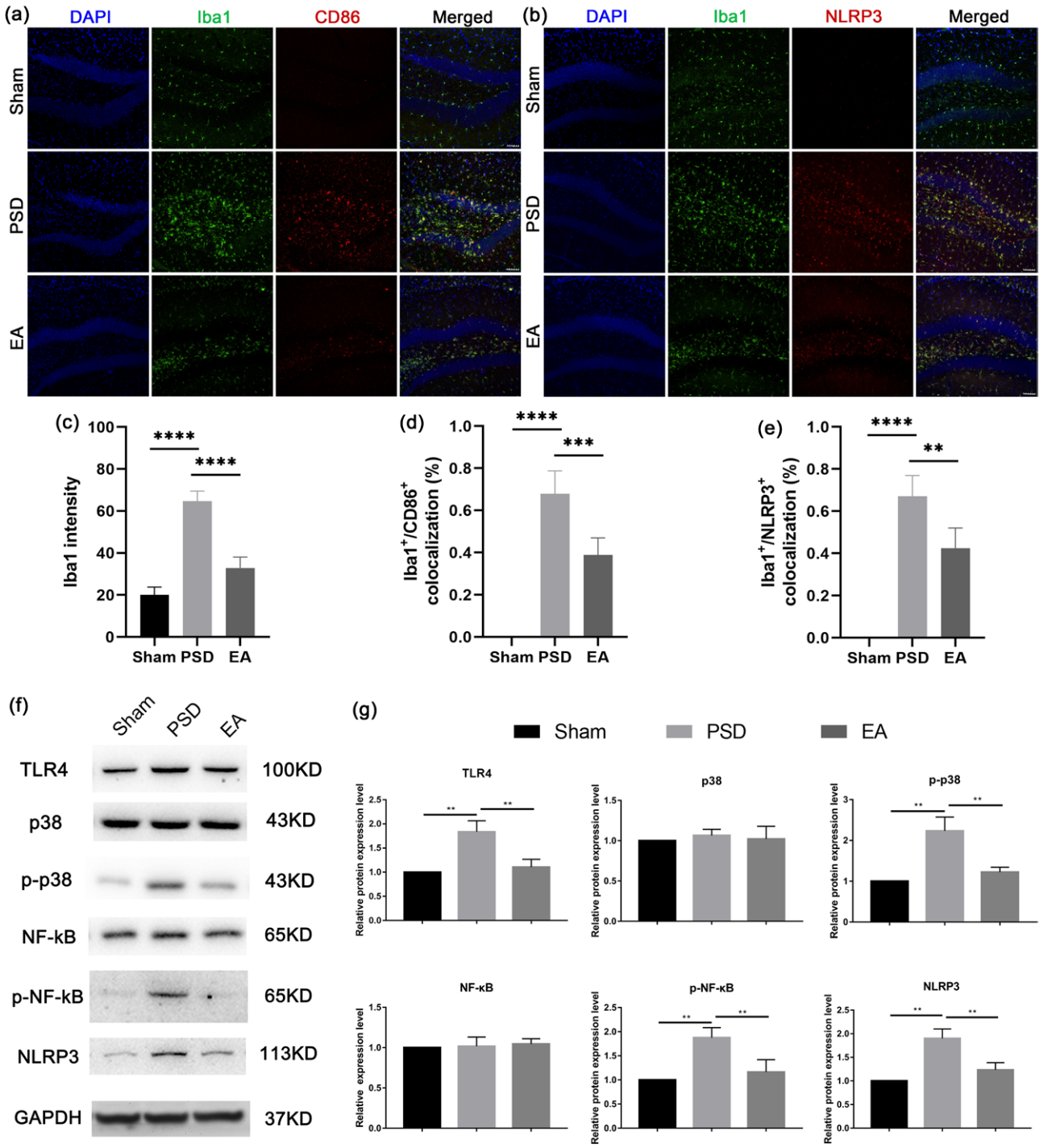


Effect of electroacupuncture on lymphocyte subsets and inflammatory cytokines in sedentary mice after ischemic stroke. (a) Representative fluorescence activated cell sorting plots of F4/80+CD11b+ macrophages gated on CD45+ cells, CD4+ cells gated on CD45+CD3+ cells, CD8+ cells gated on CD45+CD3+ cells, and CD3-CD49b+ cells gated on CD45+CD49b+ cells in the peripheral blood. Bar graph showing the percentage of F4/80+CD11b+ cells in CD45+ cells [$F(2,10) = 9.48$, $P = 0.008$] (b), CD4+ cells in CD45+CD3+ cells [$F(2,10) = 10.24$, $P = 0.008$] (c), CD8+ cells in CD45+CD3+ cells [$F(2,10) = 6.05$, $P = 0.013$] (d), the ratio of CD4+ to CD8+ cells [$F(2,10) = 30.25$, $P < 0.001$] (e), and CD3-CD49b+ cells in CD45+CD49b+ cells [$F(2,10) = 35.34$, $P < 0.001$] (f). (g) Electroacupuncture significantly increased the level of IL-1β in the ischemic hippocampus. (h) Electroacupuncture significantly increased the level of IL-6 in the ischemic hippocampus. (i) Electroacupuncture significantly increased the level of TNF-α in the ischemic hippocampus. All values are presented as means ± SD. *$P < 0.05$ and **$P < 0.01$ as determined by one-way ANOVA (Tukey's multiple comparison test, $n = 4$). ANOVA, analysis of variance.

expressed NLRP3 inflammasomes. In contrast, the hippocampal region of mice in the electroacupuncture group exhibited significantly reduced expression of Iba1/CD86 ($P < 0.001$) and Iba1/NLRP3 ($P = 0.001$) signals (Fig. 6a–e). This finding provides new insights into our understanding of the immune response mechanisms of glial cells in CNS diseases.

In previous studies, the TLR4 pathway has been identified as playing a crucial role in depression [15]. Therefore, we investigated whether electroacupuncture could regulate TLR4 activity and its downstream signal in the ischemic hippocampus. Compared with the sham group, western blotting demonstrated the levels of TLR4 ($P < 0.01$), p-p38 ($P < 0.01$), p-NF-κB ($P < 0.01$),

Fig. 6



Effects of electroacupuncture on microglia-mediated neuroinflammation in the sedentary mice after ischemic stroke. (a) Representative images of double-labeling immunostaining of Iba1/CD86 (Iba1-green and CD86-red) in hippocampal dentate gyrus (Scale bar = 60 μm). (b) Representative images of double-labeling immunostaining of Iba1/NLRP3 (Iba1-green and NLRP3-red) in hippocampal dentate gyrus (Scale bar = 60 μm). (c) Quantitative analysis of the iba1 intensity in hippocampal dentate gyrus. One-way ANOVA was used to analyze the data [F (2,10) = 125.30, $P < 0.0001$]. (d) Iba1/CD86 colocalization analysis revealed that electroacupuncture signifcantly reduced the expression of CD86 on microglia. One-way ANOVA was used to analyze the data [F (2,10) = 95.33, $P < 0.0001$]. (e) Iba1/NLRP3 colocalization analysis revealed that electroacupuncture signifcantly reduced the expression of NLRP3 on microglia. One-way ANOVA was used to analyze the data [F (2,10) = 91.18, $P < 0.0001$]. (f) Western blot assays for TLR4, p38, p-p38, NF-κB, p-NF-κB, and NLRP3 in the ischemic hippocampus. (g) The quantitative analysis for the results of TLR4, p38, p-p38, NF-κB, p-NF-κB, and NLRP3 in western blot. Four-week electroacupuncture significantly decreased TLR4, p-p38, p-NF-κB, and NLRP3 levels in the ischemic hippocampus. All values are presented as means ± SD. *$P < 0.05$, **$P < 0.01$, ***$P < 0.001$, ****$P < 0.0001$ as determined by one-way ANOVA (Tukey's multiple comparison test, $n = 4$). ANOVA, analysis of variance.

and NLRP3 ($P < 0.01$) in the ischemic hippocampus significantly increased ($P < 0.01$) after ischemic stroke with sedentary behavior. In contrast, electroacupuncture for 4 weeks significantly decreased TLR4 ($P < 0.01$), p-p38 ($P < 0.01$), p-NF-κB ($P < 0.01$), and NLRP3 levels ($P < 0.01$) compared to the PSD group (Fig. 6f–g). This evidence supports that electroacupuncture can inhibit the TLR4/p38/NF-κB/NLRP3 inflammatory pathway activated by PSD.

Discussion

In our present study, we investigated both the behavioral and molecular impacts of electroacupuncture in a rodent model of cerebral ischemia combined with sedentary behavior. Our results suggest that early administration of electroacupuncture poststroke can mitigate depressive behaviors and facilitate hippocampal neurogenesis. Additionally, this treatment fosters the persistence of newly generated neurons in the hippocampal dentate gyrus, possibly through the inhibition of TLR4/p38/NF-κB/NLRP3 signaling pathways and the improvement of the microglia-mediated neuroinflammation within the hippocampus.

Stroke poses a severe and often life-threatening threat with substantial fatality and disability rates [16]. One prevalent psychiatric aftermath of stroke is depression, often characterized by a sustained and profound dip in mood. The high morbidity rate of PSD, estimated at an alarming 31%, significantly impacts the quality of life and may lead to increased suicidal tendencies among stroke survivors [2,17]. Moreover, various chronic physical conditions such as diabetes, cancer, cardiovascular diseases, chronic pain, and respiratory diseases are frequently accompanied by depression and anxiety [18]. Depressed individuals typically exhibit reduced physical activity and persistent sedentary behavior. Recent findings suggest that imposed sedentary behavior over a week could instigate adverse mood swings, even depression, particularly in young adults [19]. Additional research has identified an elevated risk of sedentary tendencies in individuals with depression, which may contribute to conditions like cardiovascular disease and metabolic syndrome [20]. In line with these findings, our study shows that sedentary behavior poststroke can trigger depression-like behavior, as observed in mice subjected to MCAO exhibiting reduced sucrose preference and increased immobility during FST, TST, EPM, and OFT after 4 weeks of sedentary lifestyle. According to the results of gait analysis, it is noteworthy that electroacupuncture did not improve the motor ability of sedentary mice after ischemic stroke. The above results indicate that electroacupuncture may directly improve the depressive-like behavior of sedentary mice, rather than improving their motor behavior.

In recent years, notable advancements have been made in depression diagnosis and treatment. The distressing reality, however, is that one-third of depression patients remain resistant to treatment and fewer than one-third achieve remission with first-line antidepressants like SSRIs. This underscores the urgent need for effective therapeutic strategies. Emerging non-pharmacologic approaches like electroconvulsive therapy or acupuncture have demonstrated significant potential. These alternative therapies, built on the principles of nervous circuit modulation, may strengthen existing depression treatment strategies.

Electroacupuncture had protective effects against ischemic stroke and sedentary behavior induced depressive symptoms, as indicated by significant increase in sucrose preference during SPT, duration in open arm during EPM, and decrease in immobility during FST, TST, and OFT. Acupuncture may impact depression through varied mechanisms, including stimulating biochemical pathways and restoring neuronal structures. Its positive mental health effects could be linked to the ability to reduce inflammation. Previous studies established that the anti-inflammatory effects of acupuncture may be attributed to four main mechanisms: (i) cytokine release alteration, (ii) regulatory effect on excitotoxicity, (iii) downregulation of toll-like receptors, and (iv) antiapoptotic properties [5,21].

Inflammation is a crucial factor in the pathogenesis of depression and anxiety, prompting the need to explore its connection with mental health. There are two key questions: whether successful depression treatment correlates with reduced inflammation, and if anti-inflammatory therapy is an effective antidepressant, particularly for individuals with an augmented inflammatory response. Existing evidence supports affirmative answers to both questions. For example, a recent meta-analysis reported that IL-6 and C-reactive protein were most closely associated with depression among inflammatory markers [22], and were highly associated with pleasure deficiency and mental retardation symptoms. Another meta-analysis including 3212 major depression disorder (MDD) patients and 2798 healthy controls showed that MDD patients had higher levels of IL-6, TNF, IL-10, sIL-2, CCL-2, IL-13, IL-18, IL-12, IL-1RA, sTNFR-2, and low level of IFN-γ [23]. While there are no approved immune-modulating anti-depression treatments, there is evidence that traditional antidepressants have anti-inflammatory effects. The antidepressant ketamine can reverse LPS induced depression-like behavior in mice, which is related to the overexpression of NLRP3 and IL-1β in hippocampus [24]. Some studies have shown that TLR4 is closely related to the occurrence and development of depression [25]. In the present study, Our RNA-seq analysis showed that the protection against PSD after electroacupuncture was highly associated with the regulation of innate immune responses involving NOD-like receptor, Toll-like receptor, and NF-κB signaling pathways. We

also observed that the levels of IL-1β, IL-6, and TNF-α in the ischemic hippocampus were markedly increased, and the percentage of CD4+ cells in CD45+CD3+ cells, ratio of CD4+ to CD8+ cells significantly decreased in the peripheral blood after ischemic stroke with sedentary behavior. While electroacupuncture significantly reduced IL-1β, IL-6, and TNF-α levels, increased the ratio of CD4+ to CD8+ T cells and the percentage of CD3-CD49b+ cells in CD45+CD49b+ cells, probably by inhibiting the TLR4/p38/NF-κB/NLRP3 inflammatory pathway in the hippocampus.

In vivo imaging studies have demonstrated reduced hippocampal and prefrontal cortex volume in MDD patients [26], these structural alterations may result from atrophy and loss of neurons and glia. Mechanisms involve glutamate excitotoxicity, decreased neurotrophic factors and activation of apoptotic pathways [27]. Further evidence support the role of cell loss in depression comes from conditions related to tissue damage, such as stroke and traumatic brain injury, which contribute to the development of depression [28]. In addition to cell loss, dysregulated adult neurogenesis is implicated in depression pathogenesis, and it has been hypothesized that therapies aimed at enhancing neurogenesis may provide neuroprotection by inducing neuroplasticity [29]. Inflammation can impact neurogenesis through various pathways. The primary mechanism underlying the reduction in adult hippocampal neurogenesis associated with inflammation is linked to the release of proinflammatory cytokines induced by microglia, such as TNF-α, IFN-α, IL-1β, and IL-6 [30]. Studies have shown that chronic IL-1β overexpression impairs the neurite complexity of immature newborn neurons in adult male rats [31], and IL-1β regulated the proliferation and differentiation of rat brain neural precursor cells [32]. The process of neurogenesis or gliogenesis involves several steps, from the proliferation of progenitor cells to the maturation of newly generated cells, and the establishment of appropriate synaptic connections, ultimately integrating into preexisting networks. In our study, the Edu labeling, doublecortin immunofluorescence staining, and Nissl staining were used to express the proliferation, differentiation, and migration of neural progenitor cells and the survival of newborn neurons, respectively. Using Golgi staining to demonstrate the branching morphology and structure of hippocampal neurons. In line with previous studies, electroacupuncture significantly enhanced the neurogenesis and prevented cell loss in the dentate gyrus. The continuous generation of new neurons in dentate gyrus plays a key role in shaping animal cognition and emotional behavior [33].

Conclusion

In conclusion, this study provides compelling evidence for the efficacy of electroacupuncture in treating PSD. Its effectiveness is attributed to anti-inflammatory properties and the promotion of hippocampal neurogenesis. Neuroinflammation and hippocampal neurogenesis play pivotal roles in depression onset and progression, mutually influencing each other. Long-term electroacupuncture reverses depression-like behaviors, promotes hippocampal neurogenesis, and fosters the survival of newborn neurons in the dentate gyrus. This process is likely achieved by inhibiting the TLR4/p38/NF-κB/NLRP3 signaling pathways and improving the microglia-mediated neuroinflammation microenvironment within this vital brain region. Future research should explore whether different acupoints and durations of electroacupuncture yield varying effects on inflammation and hippocampal neurogenesis. This is crucial because it may have different or opposite effects on the treatment of PSD or other forms of disease-related depression.

Acknowledgements

This study was supported by the Natural Science Foundation of Gansu province (21JR11RA151, 22JR5RA 609, 23JRRA1584).

The protocol of animal care and experiments were approved by the Ethical Review Board of Gansu University of Chinese Medicine. The protocols of these animals were followed the National Institutes of Health Guide for the Care and Use of Laboratory Animals.

All data analyzed and presented in this study are available from the corresponding author on reasonable request.

Conflicts of interest

There are no conflicts of interest.

References

1 Richards CL, Malouin F, Nadeau S. Stroke rehabilitation: clinical picture, assessment, and therapeutic challenge. *Prog Brain Res* 2015; **218**:253–280.
2 Dou DM, Huang L-L, Dou J, Wang X-X, Wang P-X. Post-stroke depression as a predictor of caregivers burden of acute ischemic stroke patients in China. *Psychol Health Med* 2018; **23**:541–547.
3 Espárrago Llorca G, Castilla-Guerra L, Fernández Moreno MC, Ruiz Doblado S, Jiménez Hernández MD. Post-stroke depression: an update. *Neurologia* 2015; **30**:23–31.
4 Hetrick S, Merry S, McKenzie J, Sindahl P, Proctor M. Selective serotonin reuptake inhibitors (SSRIs) for depressive disorders in children and adolescents. *Cochrane Database Syst Rev* 4851; **2007**:Cd00.
5 Yang NN, Lin L-L, Li Y-J, Li H-P, Cao Y, Tan C-X, *et al*. Potential mechanisms and clinical effectiveness of acupuncture in depression. *Curr Neuropharmacol* 2022; **20**:738–750.
6 Yang A, Wu HM, Tang J-L, Xu Li, Yang M, Liu GJ. Acupuncture for stroke rehabilitation. *Cochrane Database Syst Rev* 2016; **2016**:CD004131.
7 Kraus C, Castrén E, Kasper S, Lanzenberger R. Serotonin and neuroplasticity - links between molecular, functional and structural pathophysiology in depression. *Neurosci Biobehav Rev* 2017; **77**:317–326.
8 Chan SW, Harmer CJ, Norbury R, O'Sullivan U, Goodwin GM, Portella MJ. Hippocampal volume in vulnerability and resilience to depression. *J Affect Disord* 2016; **189**:199–202.
9 Lamers F, Milaneschi Y, de Jonge P, Giltay EJ, Penninx BWJH. Metabolic and inflammatory markers: associations with individual depressive symptoms. *Psychol Med* 2018; **48**:1102–1110.
10 Yang J, Liu R, Lu F, Xu F, Zheng J, Li Z, *et al*. Fast green FCF attenuates lipopolysaccharide-induced depressive-like behavior and downregulates

TLR4/Myd88/NF-kappaB signal pathway in the mouse hippocampus. *Front Pharmacol* 2019; **10**:501.
11 Guo LT, Wang S-Q, Su J, Xu L-X, Ji Z-Y, Zhang R-Y, *et al*. Baicalin ameliorates neuroinflammation-induced depressive-like behavior through inhibition of toll-like receptor 4 expression via the PI3K/AKT/FoxO1 pathway. *J Neuroinflammation* 2019; **16**:95.
12 Lu YC, Yeh WC, Ohashi PS. LPS/TLR4 signal transduction pathway. *Cytokine* 2008; **42**:145–151.
13 Hong C, Chen L, Kong W, Zhang D, Wang L, Zhao J, *et al*. Behavioral and neurochemical changes in rats with recurrent depression induced by chronic unpredictable stress. *Neuro Endocrinol Lett* 2021; **42**:387–394.
14 Yu F, Huang T, Ran Y, Li D, Ye L, Tian G, *et al*. New insights into the roles of microglial regulation in brain plasticity-dependent stroke recovery. *Front Cell Neurosci* 2021; **15**:727899.
15 Amiresmaeili A, Roohollahi S, Mostafavi A, Askari N. Effects of oregano essential oil on brain TLR4 and TLR2 gene expression and depressive-like behavior in a rat model. *Res Pharm Sci* 2018; **13**:130–141.
16 Daglia M, Di Lorenzo A, Nabavi SF, Sureda A, Khanjani S, Moghaddam AH, *et al*. Improvement of antioxidant defences and mood status by oral GABA tea administration in a mouse model of post-stroke depression. *Nutrients* 2017; **9**:446.
17 Stern-Nezer S, Eyngorn I, Mlynash M, Snider RW, Venkatsubramanian C, Wijman CAC, *et al*. Depression one year after hemorrhagic stroke is associated with late worsening of outcomes. *NeuroRehabilitation* 2017; **41**:179–187.
18 Freedland KE, Carney RM. Depression as a risk factor for adverse outcomes in coronary heart disease. *BMC Med* 2013; **11**:131.
19 Edwards MK, Loprinzi PD. Effects of a sedentary behavior-inducing randomized controlled intervention on depression and mood profile in active young adults. *Mayo Clin Proc* 2016; **91**:984–998.
20 Schuch F, Vancampfort D, Firth J, Rosenbaum S, Ward P, Reichert T, *et al*. Physical activity and sedentary behavior in people with major depressive disorder: a systematic review and meta-analysis. *J Affect Disord* 2017; **210**:139–150.
21 Cai W, Shen WD. Anti-apoptotic mechanisms of acupuncture in neurological diseases: a review. *Am J Chin Med* 2018; **46**:515–535.
22 Haapakoski R, Mathieu J, Ebmeier KP, Alenius H, Kivimäki M. Cumulative meta-analysis of interleukins 6 and 1β, tumour necrosis factor α and C-reactive protein in patients with major depressive disorder. *Brain Behav Immun* 2015; **49**:206–215.
23 Köhler CA, Freitas TH, Maes M, de Andrade NQ, Liu CS, Fernandes BS, *et al*. Peripheral cytokine and chemokine alterations in depression: a meta-analysis of 82 studies. *Acta Psychiatr Scand* 2017; **135**:373–387.
24 Li JM, Liu L-L, Su W-J, Wang B, Zhang T, Zhang Y, *et al*. Ketamine may exert antidepressant effects via suppressing NLRP3 inflammasome to upregulate AMPA receptors. *Neuropharmacology* 2019; **146**:149–153.
25 Porcu M, Urbano MR, Verri WA, Barbosa DS, Baracat M, Vargas HO, *et al*. Effects of adjunctive N-acetylcysteine on depressive symptoms: modulation by baseline high-sensitivity C-reactive protein. *Psychiatry Res* 2018; **263**:268–274.
26 Sheline YI. 3D MRI studies of neuroanatomic changes in unipolar major depression: the role of stress and medical comorbidity. *Biol Psychiatry* 2000; **48**:791–800.
27 Banasr M, Dwyer JM, Duman RS. Cell atrophy and loss in depression: reversal by antidepressant treatment. *Curr Opin Cell Biol* 2011; **23**:730–737.
28 Robinson RG, Jorge RE. Post-stroke depression: a review. *Am J Psychiatry* 2016; **173**:221–231.
29 Krishnan V, Nestler EJ. The molecular neurobiology of depression. *Nature* 2008; **455**:894–902.
30 Monje ML, Toda H, Palmer TD. Inflammatory blockade restores adult hippocampal neurogenesis. *Science* 2003; **302**:1760–1765.
31 Hueston CM, O'Leary JD, Hoban AE, Kozareva DA, Pawley LC, O'Leary OF, *et al*. Chronic interleukin-1β in the dorsal hippocampus impairs behavioural pattern separation. *Brain Behav Immun* 2018; **74**:252–264.
32 Wang X, Fu S, Wang Y, Yu P, Hu J, Gu W, *et al*. Interleukin-1beta mediates proliferation and differentiation of multipotent neural precursor cells through the activation of SAPK/JNK pathway. *Mol Cell Neurosci* 2007; **36**:343–354.
33 Kheirbek MA, Hen R. Dorsal vs ventral hippocampal neurogenesis: implications for cognition and mood. *Neuropsychopharmacology* 2011; **36**:373–374.